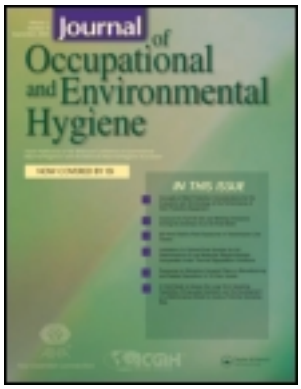

Journal of Occupational and Environmental Hygiene
Publication details, including instructions for authors and subscription information:
http://www.tandfonline.com/loi/uoeh20

Evaluation of Respirator Filters for Asbestos Fibers

Yung-Sung Cheng [a], Thomas D. Holmes [a] & Bijian Fan [b]
[a] Lovelace Respiratory Research Institute, Albuquerque, New Mexico
[b] Amgen Inc., Thousand Oaks, California
Published online: 24 Oct 2007.

To cite this article: Yung-Sung Cheng, Thomas D. Holmes & Bijian Fan (2006) Evaluation of Respirator Filters for Asbestos Fibers, Journal of Occupational and Environmental Hygiene, 3:1, 26-35, DOI: 10.1080/15459620500444046

To link to this article: http://dx.doi.org/10.1080/15459620500444046

Journal of Occupational and Environmental Hygiene, 3: 26–35
ISSN: 1545-9624 print / 1545-9632 online

DOI: 10.1080/15459620500444046

Evaluation of Respirator Filters for Asbestos Fibers

Yung-Sung Cheng,[1] Thomas D. Holmes,[1] and Bijian Fan[2]

[1]Lovelace Respiratory Research Institute, Albuquerque, New Mexico
[2]Amgen Inc., Thousand Oaks, California

Fiber aerosols are known to have different aerodynamic behaviors than spherical particles and usually carry higher electrostatic charges. We investigated the effects of flow rate and charge status of filter cartridges on the penetration of spherical and fiber aerosols. Four types of test respirator filters were selected: two for passive respirators, one for a powered respirator, and one disposable respirator. Surface charges on respirator filters were determined using a noncontact field electrostatic field meter. Penetration tests were performed for filter cartridges before and after charge neutralization. The surface charge measurements on the respirator filters showed that some filters, including those used in disposable face masks, are charged to enhance the collection efficiency. Only high-efficiency particulate air filters performed consistently for both spherical test aerosols and the three types of asbestos fibers. The surface charge potential of filter cartridges and flow rate did not appear to affect the performance of these filters. In contrast to the high-efficiency filters, the aerosol penetration performance of low-efficiency filters and face masks deteriorated when the charge potential on the filter was removed. Our data also showed that the surface charges decreased in a high-temperature, high-humidity environment and disappeared after 1 week. Deposition of spherical particles and fibers in the charged disposable facemask filter was enhanced. For charged-neutralized, low-efficiency filter cartridges, asbestos fibers may penetrate more than spherical particles with a mean particle size of 0.3 μm diameter.

Keywords asbestos, disposal mask, filter penetration, respirator cartridge

Address correspondence to: Yung-Sung Cheng, Lovelace Respiratory Research Institute, 2425 Ridgecrest Drive SE, Albuquerque, NM 87108. E-mail: ycheng@lrri.org.

Exposure to asbestos fibers by inhalation may lead to primary lung cancers, mesothelioma, and pulmonary and pleural fibrosis. The carcinogenic potential of asbestos fibers has been shown to correlate with fiber dimensions and their durability in the lungs.[1,2] Concerns about the health risks associated with exposure to asbestos fibers have resulted in restricting their use in many applications, including thermal insulation and construction materials. However, many public buildings and private residences that contained asbestos as building or insulation material now require removal of the asbestos.

Man-made fibrous materials, such as fiberglass and ceramic fibers, have been developed to replace asbestos. Silicon carbide, silicon nitride, and other fibers are important constituents of composite materials that have applications in aerospace and automotive industries.[3] Health effects of inhalation exposures to these man-made fibers have been evaluated.[4–6] Potential sources of exposure to fibrous materials in occupational environments will continue to increase with expansion of commercial applications.

The Occupational Safety and Health Administration (OSHA) has set the permissible exposure limit (PEL) for asbestos fibers at 0.1 fibers mL^{-1} of air in occupational environments.[7] Engineering controls and work practices are the preferred methods to reduce worker exposure in these environments. However, if these methods cannot reduce the asbestos concentration below the PEL, then respiratory protection is required to minimize exposure. The OSHA guidelines also require respiratory protection during maintenance and repair activities and in emergencies.

Fiber particles with elongated shapes (ratio of length to diameter >3:1) have aerodynamic characteristics that are different from spherical particles of the same volume and density. The aerodynamic behavior of fibrous aerosols is largely dependent on the diameter of the fiber, with the length of the fiber having a minor influence.[3,8,9] Asbestos fibers found in most occupational environments have wide size distributions in both diameter and length.[10] The diameter of respirable asbestos fibers ranges from 0.01 μm to 3.0 μm, and the length ranges from 0.1 μm to 60 μm.[10] Man-made fibers, such as glass, ceramic, and carbon, have a diameter between 0.1 μm to 10 μm and an aspect ratio ranging from 3 to 60. Because of the wide size range of fiber aerosols, it is essential that a respirator certified for use on one type of fiber is also suitable for other types of fiber aerosols with potentially very different size characteristics.

Data are limited on fiber filtration through respirator filters. Weeks and Burns[11] reported 0% to 2.6% penetration of a chrysotile asbestos aerosol through eight different respirator filters. Brosseau et al.[12] reported 0.01% to 0.1% mean

penetration of an amosite aerosol at 32 L min^{-1} constant flow and mean penetration of 0.1 to 0.6% at 76 L min^{-1} cyclic flow. They also tested the same filters with silica aerosols.

Ortiz et al.[13] compared the penetration of chrysotile asbestos and an oil test aerosol of di-(2-ethylhexyl) sebacate (DEHS) through filter cartridges approved by the National Institute for Occupational Safety and Health (NIOSH).[14] A lower penetration rate (0% to 3%) was observed for asbestos than for DEHS aerosols (0% to 30%) when the filters were taken from the package without extended storage time. However, after a 1-week storage at a high temperature (38°C) and in high humidity (90% +), the fiber penetration increased to 20% for some filters. Similar deterioration of filter performance was found after filters received a substantial particle load of DEHS or were instilled with water mist. This level of fiber penetration (20%) could certainly result in workers being exposed to fiber concentrations that exceed the PEL in work environments with >0.5 fibers mL^{-1} concentration, even if they wore respirators. The only filter that performed consistently under all conditions was a high-efficiency particulate air (HEPA) filter.

These studies reported the overall penetration of one type of asbestos that may not be applicable to other types of asbestos because of different fiber dimensions. On the other hand, electrostatic charges associated with filter cartridges have been implicated in the inconsistent results of filter performance reported by Ortiz et al.,[13] but their experimental design did not provide sufficient information to test this hypothesis. In this study we used three types of asbestos fibers and spherical DEHS particles as test materials. The effects of surface charge potential and flow rate on fiber penetration were also studied.

The objectives of our research were to (a) quantify the performance of respirator filters used to protect workers in environments where they may be at risk for exposure to asbestos and man-made fibers, and (b) to elucidate the mechanical and electrical deposition mechanisms for the filtration of fiber aerosols. This information will help to determine which types of fiber aerosols are most likely to penetrate the respirable filters and to predict the performance of respirator filters under different field conditions.

This article describes the experimental approaches for investigating electrostatic charges of filters and penetration of asbestos fibers, including amosite, crocidolite, and chrysotile through several commercially available respirator filters. Penetration tests were also performed using the spherical DEHS aerosol according to the NIOSH test procedures. A direct comparison of the filter performance between the fiber aerosols and spherical aerosols was made. Some filter cartridges consisting of materials of low conductivity may carry electrostatic charges; these charges may be lost during storage under conditions of high temperature and high humidity. Surface potential of filter cartridges were measured to ascertain the effects of temperature and humidity. Fiber penetration through filters fresh from the package and stored under these conditions was studied.

MATERIALS AND METHODS

Characterization of Test Filters

Four types of respirator filters were used in the study: (1) a disposable, low-efficiency face mask filter (3M8710; 3M, St. Paul, Minn.); (2) a dust/fume/mist filter cartridge (Type S; MSA, Pittsburgh, Pa.); (c) a HEPA filter for powered respirators (Type A, MSA); and (d) a HEPA filter (AOR57A; American Optical Corp., Southbridge, Mass.), as shown in Table I. Following NIOSH test procedures, Filters D and B, which are used in dual cartridges, were tested at 16 and 42.5 L min^{-1}using a single cartridge; Filters A and C were tested at 32 and 85 L min^{-1}. Filter A was attached to the test filter adapter ring with a bead of silicone adhesive. The edges of the filter were trimmed close to the adapter ring and sealed with adhesive. The adapter ring was then attached to the main filter adapter with vinyl tape.

Filter Surface Charge Potential Measurements

The hypothesis postulated was that an increased electrical charge status on a filter cartridge would increase the efficiency of the filter. To test this hypothesis, filter cartridges were used directly from the box and after treatment with an antistatic fluid (Zero Charge; Tech Spray, Amarillo, Texas). The surface charge potential on the filters before and after the treatment was measured with an electrostatic field meter (model 245; Monroe Electronics, Lyndonville, N.Y.). The meter was carefully placed on a movable table with a nonconducting surface (Daedal Inc., Harrison City, Pa.). The probe of the field meter was placed about 5 cm from the surface to measure the electrical field charge. Measured values of nine equally spaced locations on the filter surface were obtained and the mean value determined.

TABLE I. Test Filter Model

Filter Code	Type	Manufacturer	Model Number	Solid Volume Fraction	Fiber Diameter (μm)
A	Disposable face mask	3M (St. Paul, Minn.)	8710	0.114	3.89
B	Dust/fume/mist	MSA (Pittsburgh, Pa.)	Type S	0.044	2.12
C	Powered respirator	MSA (Pittsburgh, Pa.)	Type A	0.056	0.51
D	HEPA	American Optical Corp., (Southbridge, Mass.)	57 A	0.064	0.30

Respirators are not as efficient under high-temperature, high-humidity conditions.[13] However, the mechanism triggering the decreased performance has not been elucidated. We hypothesized that this deficiency was related to the electrostatic charge status of the filter. To test this, we placed new filter cartridges in an oven (model 5851; National Appliance Co., Portland, Ore.) maintained at 38°C and >90% relative humidity for up to 11 days. The filters were taken out from time to time for surface charge potential measurement.

Test Materials

Three asbestos fibers of different diameters were tested: an ultrafine chrysotile (Calidria), a UICC crocidolite, and a UICC amosite.[15,16] The wide range of fiber diameters and lengths was important to examine as a direct interception mechanism. Penetration tests with the same respirator filters were performed using the DEHS (Sigma Chemical Co., St. Louis, Mo.) aerosol according to NIOSH test procedures. The overall penetration was estimated by measuring upstream and downstream concentrations. A direct comparison of the filter performance between the fiber aerosols and the spherically shaped DEHS aerosols was obtained.

Spherical Particle Penetration of the Filters

The experimental setup for measuring fractional penetration of DEHS aerosols in the test respirator filters is shown schematically in Figure 1. A condensation aerosol generator (model 3076; TSI, St. Paul, Minn.) was used.[17] DEHS was dissolved in isopropanol and delivered by a syringe pump at a flow rate of 0.75 $cm^3\,s^{-1}$ to a nebulizer in order to produce droplets. The droplets were heated for evaporation in the heating column, and the DEHS vapor condensed to form submicrometer aerosols. The particles then moved at a flow rate of 3.5 $L\,min^{-1}$ through a ^{85}Kr discharger, which lowered their charge to the Boltzmann equilibrium charge level. The neutralizer tube was placed inside an active carbon absorber, which absorbed the isopropanol. The flow rate was increased prior to the particles reaching the test chamber in order to meet test requirements.

A mixing fan was placed inside the cone located before the chamber to increase aerosol uniformity. A honeycomb flow straightener was placed between the fan and the chamber to reduce the turbulence. The test chamber was a cylinder (31 cm inner diameter × 43 cm long); flow in the test chamber was laminar, and the aerosol concentration was uniform.

Prefilter and postfilter probes were located in the test chamber to sample the aerosols. A pressure gauge measured the pressure differential across the test filter. A change in pressure indicated that aerosol particles had built up on the filter. A real-time aerosol monitor (RAM-1; MIE Inc., Bedford, Conn.) was connected to the sample probes and measured the mass concentrations before and after the filter. A quartz crystal microbalance (QCM) cascade impactor (model PC-2; California Measurements Inc., Sierra Madre, Calif.) was used to determine the aerosol size distribution.

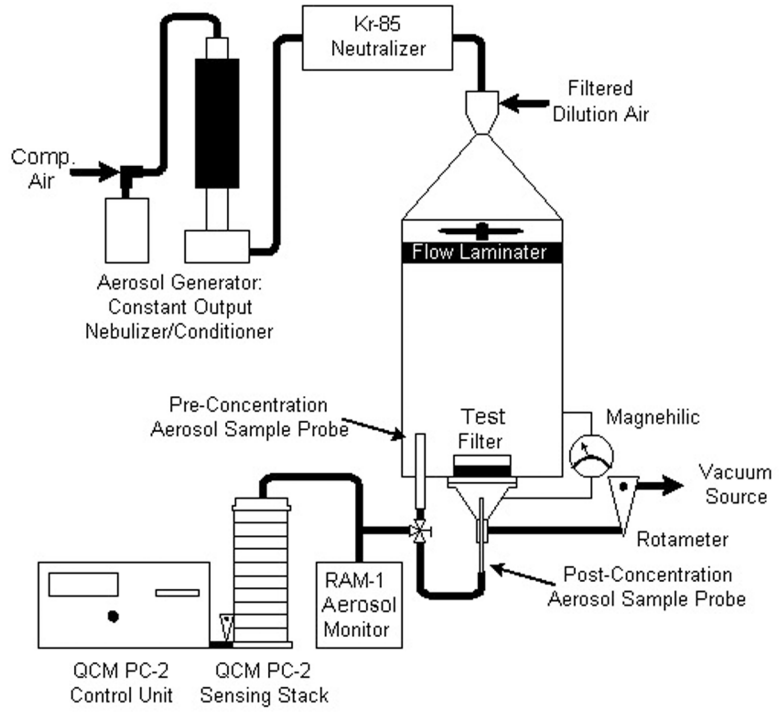

FIGURE 1. Experimental setup for measuring fractional penetration of DEHS aerosol spherical particles.

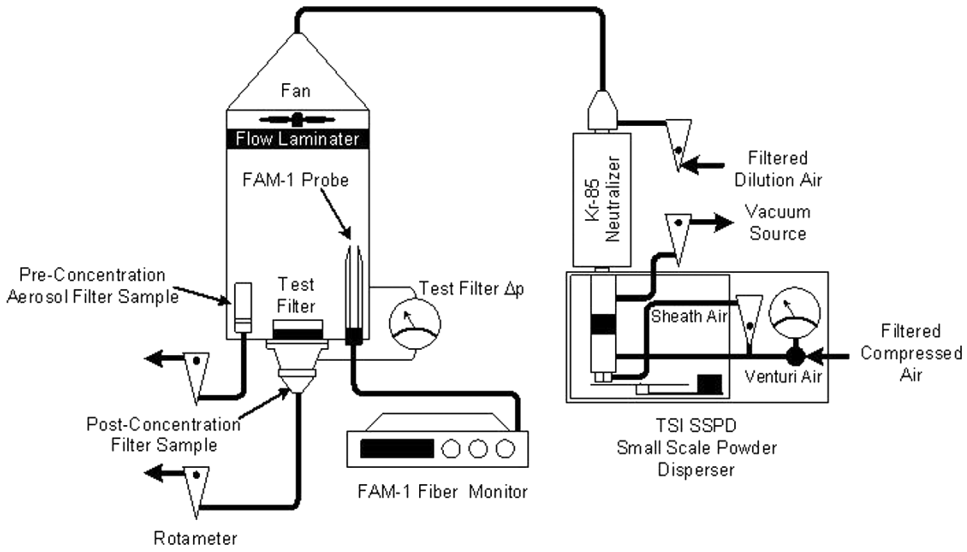

FIGURE 2. Experimental setup for asbestos fibers.

Penetration of Asbestos Fibers in the Filter

Figure 2 shows the experimental apparatus used in the filter penetration studies. Amosite and crocidolite fiber aerosols were generated by a small-scale powder disperser (SSPD, model 3433; TSI Inc.). The SSPD consisted of a rotational disk coated with powder and a suction tube to collect the fibers from the disk and disperse them as an aerosol.[3,18] The aerosol was delivered at a flow rate of 22.5 L min^{-1}. Fine chrysotile fibers were generated by nebulization. The powder was washed and suspended in methanol. The suspension was then nebulized using a Retec nebulizer (InTox Inc., Albuquerque, N.M.).

The aerosol was passed into an ^{85}Kr discharger tube to neutralize the fibers, through a dilutor to maintain proper concentration, and into the test chamber where a small fan and flow straightener distributed the flow evenly. The test chamber was the same unit used for the DEHS penetration experiments described earlier. A fiber air monitor (FAM-1; MIE Inc., Billerica, Mass.) served as a real-time monitor for fiber concentration flowing through the chamber. An asbestos filter sampler with conductive material (Millipore Corp., Bedford, Mass.) was used to collect samples in the test chamber for initial fiber concentrations. The filter cartridge was placed in a test assembly. Fibers that penetrated the cartridge were collected in a filter downstream of the test assembly. Twenty-five mm and 47-mm membrane filters (mixed cellulose acetate and nitrate, Millipore) were used in upstream and downstream samplers.

The flow rate through the asbestos filter sampler was 1 L min^{-1}, whereas the flow rate for the downstream filter sampler was 16, 32, 42.5, or 85 L min^{-1}, the same flow rate as through the test respiratory filter. The pressure in the test chamber and the pressure drop across the test cartridge were monitored to verify that the desired flow rates were maintained. Each type of fresh filter cartridge was tested for all three fibers and fiber penetration were retested for filter cartridges treated with the antistatic spray.

Fiber collection under three experimental conditions was studied. At a flow rate of 32 L min^{-1} for single cartridges (Filters A and C) or 16 L min^{-1} for dual cartridges (Filters B and D), two conditions were studied: (1) untreated filter with charge-neutralized fibers, and (2) filter treated to remove charges with charge-neutralized fibers. These sets of data were intended to investigate the influence of charge status on filter cartridges. To investigate the effects of flow rate, experiments were also conducted for a higher flow rate of 85 L min^{-1} for Filters A and C, or 42.5 L min^{-1} for dual cartridges (Filters B and C). In this case, the filters were treated to remove charges and the fibers were neutralized also.

Fiber Sample Preparation

The generator, chamber, filter, and samplers for fiber experiments were housed in a vented glovebox enclosure. Filter samples were taken to determine aerosol concentration and diameter/length distribution. Filter samples were coated with carbon in a vacuum coating plant. Copper electron microscope (EM) grids were placed on top of the filter substrate attached to the carbon film. The filter was then placed in acetone for 20 min to dissolve the filter substrate.

The grids were examined and photographed in a Hitachi-7000 Scanning Transmission EM (STEM; Hitachi Ltd., Tokyo, Japan) at a magnification of 2000. The photographic negatives were enlarged to a final magnification of 6000. A series of 10 to 20 photographs was taken to cover a certain area of grid space. These photographs were then placed together. Individual fibers in the viewing area were counted, and the length and diameter for each fiber was measured with an electronic digital caliper (MAX-CAL; Cole-Parmer Instrument, Niles, Ill.). Only fibers with aspect ratios > 3.0 were considered in the efficiency calculations. Approximately 200 to 600 individual fibers from

each montage were measured to derive a diameter/length distribution for the upstream fiber samples.

Determination of Fiber Concentration

For each sample, the number of fibers in each diameter and length interval was entered into a table. The number concentrations can be calculated from the sum of fiber counts (N) in the viewing area (A), the sampling volume (V), and the total filter area (A_t):

$$C = \frac{NA_t}{AV} \quad (1)$$

This formula assumes that fiber collection on a given filter sample was uniformly distributed. Flow and particle concentration profiles in the downstream filter collection were calculated to determine the validity of this assumption. A computational fluid dynamic package, FIDAP (Fluid Dynamics International, Evanston, Ill.), was used to numerically solve the governing equations for concentration and flow. Figure 3 shows the schematic diagram of the 47-mm membrane filter sampler used to collect all fibers penetrating the test respirator filter. The flow profile inside the sampler and upstream of the collection filter is plotted in Figure 4. Our results suggested that the velocity and concentration profiles were nearly uniform across the collecting surface except near the wall, where they decreased to zero. Based on the calculated concentration and velocity profiles, we concluded that Equation 1 was valid if samples for EM grids were taken in most areas of the sample filters. We decided to take samples from areas close to the center.

Fiber Size Distributions

From the measured length and diameter for each fiber, a diameter/length matrix can be established for each sample taken during the experiment. The distribution can be expressed as a bivariate lognormal distribution if the diameter and length distributions can be shown to follow lognormal distribution.[8] Figures 5 and 6 show examples of the cumulative length and diameter distributions plotted in log-probability scale for amosite fibers from one experiment. The straight line of cumulative distributions in the log-probability scale is indicative of a log-normal distribution. Data for other fibers were similar (data not shown). Therefore, we can express the probability density function of the fiber length/width distribution, $f(L,D) = \frac{dn}{n_o d\log(L) d\log(d)}$ as:

$$f(L,d) = \frac{1}{2\pi\beta_L\beta_D(1-\tau^2)^{0.5}} \exp\left[-\frac{A^2 + B^2 - 2\tau AB}{2(1-\tau^2)}\right]$$
$$A = \frac{(\ln d - \mu_D)}{\beta_D}$$
$$B = \frac{(\ln L - \mu_L)}{\beta_L} \quad (2)$$
$$\tau = \frac{\beta_{LD}}{\beta_L\beta_D}$$
$$\beta_{LD} = \frac{1}{N-1}\Sigma_{i=1}^{K}\Sigma_{j=1}^{M}(\ln L - \mu_L)(\ln d_j - \mu_D)$$

where μ_L and μ_D are the natural logs of the count median length and diameter (CML and CMD), and β_L and β_D are the

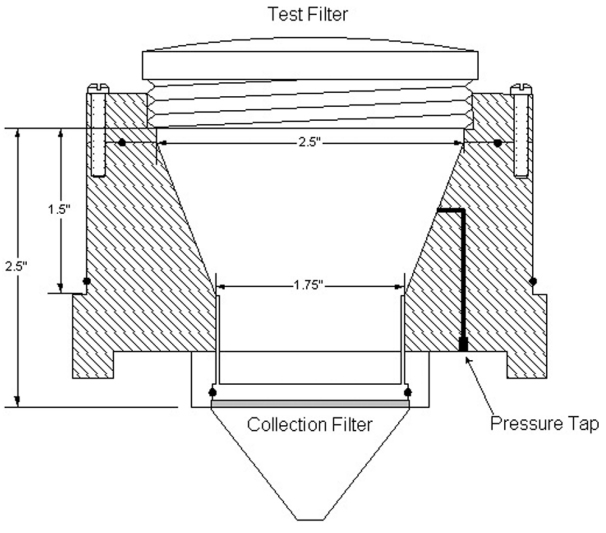

FIGURE 3. Test filter assembly. The test assembly was made of aluminum.

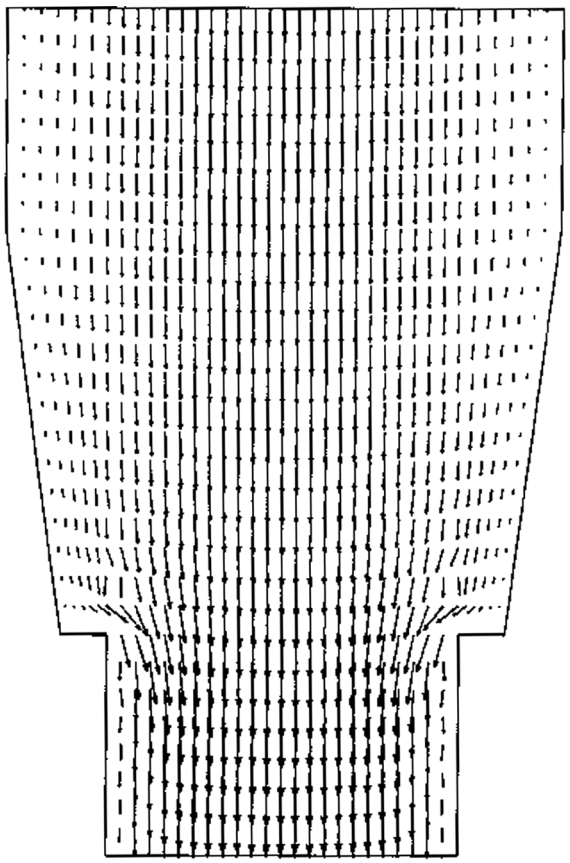

FIGURE 4. Stream line of flow in the test filter assembly.

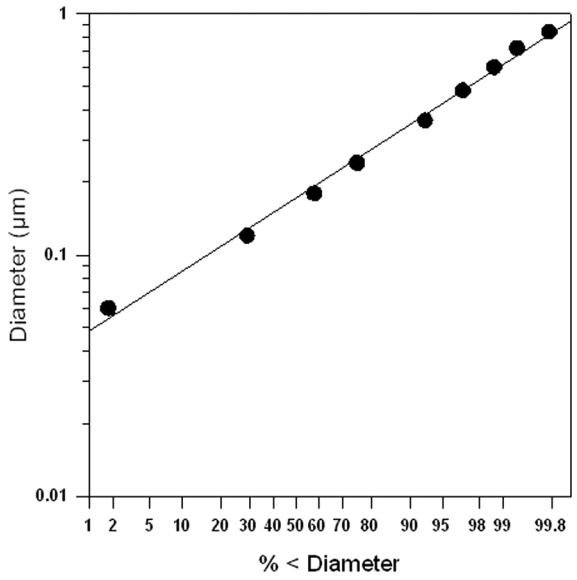

FIGURE 5. Cumulative distribution of amosite diameter.

natural log of the geometric standard deviations (σ_g) for length and diameter.

Determination of Fiber Penetration

From our data, both the overall and size-specific penetrations of a fiber through each test filter can be obtained. The overall penetration is defined as the ratio of the fiber concentration leaving the test filter (C) and the initial concentration (C_o):

$$P_t = \frac{C}{C_o} \quad (3)$$

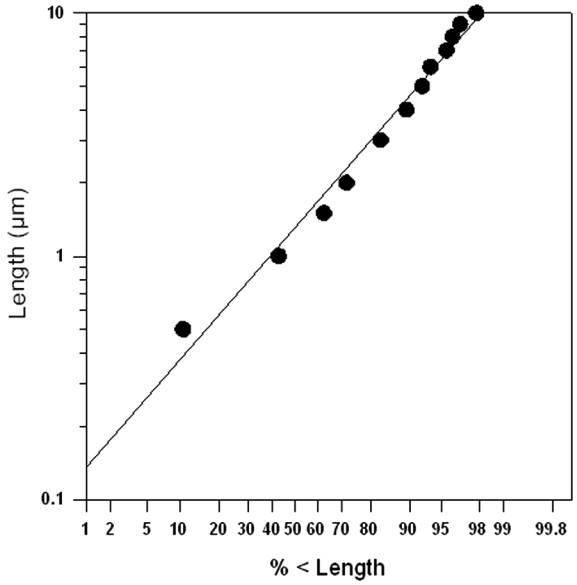

FIGURE 6. Cumulative distribution of amosite length.

The fiber concentrations C and C_o were calculated from upstream and downstream samples.

RESULTS AND DISCUSSION

Surface Charge Potential on Filter Cartridges

Negative surface charge potentials were detected in all four types of filter cartridges. Filters A and C had higher potentials between 800 and 1800 volts, whereas two other types of cartridges had much lower potentials of around 20 volts. The charge potential varied between individual cartridges of the same type. Treatment with antistatic fluid removed all surface potentials. Figure 7 shows the effects of conditioning under high temperature and humidity. Our data showed that surface charge potentials were reduced substantially within 2 days, and by Day 6 most surface charges were removed.

Penetration of the DEHS Aerosol

The DEHS aerosol generated in this study had a mass median aerodynamic diameter of 0.30 μm and σ_g of 1.27 based on the QCM impactor measurement. The aerosol collection efficiencies and in the filter cartridge and face mask are shown in Table II. The effects of flow rate and filter treatment on the collection efficiency of the low-efficiency face mask (Filter A) and the dust/fume/mist filter (Filter B) were similar. In terms of the differences in percentage deposition, charge status on the filter played an important role in increasing the efficiency of the filter, whereas flow rate had a very small effect on the efficiency

TABLE II. DEHS Aerosol Deposition in the Respirator Filter

Filter Type	Filter Treatment	Flow Rate (L min^{-1})	Aerosol Deposition (%)	
			Mean[A]	SD[A]
Filter A	Untreated	32	84.63	0.0168
Filter A	Neutralized	32	43.96	0.0060
Filter A	Untreated	85	78.17	0.92
Filter A	Neutralized	85	34.93	0.89
Filter B	Untreated	16	95.21	0.02
Filter B	Neutralized	16	94.68	0.05
Filter B	Untreated	42.5	94.45	0.08
Filter B	Neutralized	42.5	93.92	0.11
Filter C	Untreated	32	99.99	0.01
Filter C	Neutralized	32	99.99	0.01
Filter C	Untreated	85	99.99	0.01
Filter C	Neutralized	85	99.99	0.01
Filter D	Untreated	16	>99.99	0
Filter D	Neutralized	16	>99.99	0
Filter D	Untreated	42.5	>99.99	0
Filter D	Neutralized	42.5	>99.99	0

Note: DEHS = di-(2-ethylhexyl) sebacate.
[A]Mean and standard deviation of three replicates.

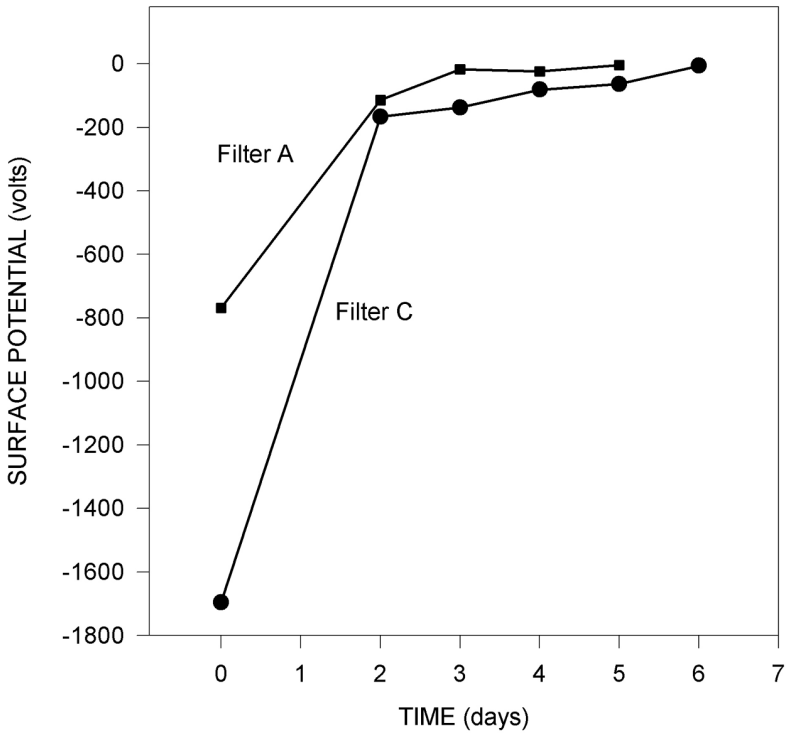

FIGURE 7. Changes of surface charge in Filters A and C at 38°C and >90% relative humidity.

of the filter. Filter B achieved 95% efficiency at 16 L min^{-1} with an untreated cartridge. The collection efficiency decreased to 94.7% when the cartridge was neutralized. Slightly lower efficiency (94.5%) was observed at 42.5 L min^{-1}, and the efficiency decreased further to 93.9% when the cartridge was neutralized. The collection efficiency was the lowest for Filter A, with 84.6% and 78.2% at 32 and 85 L min^{-1}, respectively. These efficiencies were substantially reduced to 44.0% and 34.9%, respectively, when neutralized cartridges were used. The treatment of the filter cartridge had a more significant effect on Filter A than on Filter B because Filter A had a higher surface charge potential, whereas the other filter had minimum surface potential.

Both Filters C and D (HEPA filters) had efficiencies >99.97%. These filters were considerably more efficient than Filters A and B. The differences between the discharged and untreated filter cartridges were negligible. The flow rate also had little influence on filter performance.

Our results confirmed that both high-efficiency filters indeed had >99.97% collection of 0.3 μm oil droplets, whereas the dust/fume/mist filter performed slightly less than the required 95% efficiency, especially when the cartridge was discharged.

Fiber Size Distribution

Figure 8 shows photos of amosite collected in samples taken upstream and downstream of a test filter. The measured size and diameter information for each test was compiled into a matrix. The cumulative distributions of diameter and length could be fitted into straight lines in a log-probability scale, an indication that the size distribution of these fibers can be expressed as bivariate lognormal distributions. The CMD, CML, diameter standard deviation (σ_{gD}), and length standard deviation (σ_{gL}) for each type of asbestos fibers obtained in the test chamber upstream of the test filter were calculated and are listed in Table III. This information indicated that the three asbestos fibers had different size/diameter distributions, which can be utilized to investigate the filter penetration

Fiber Collection/Penetration

Total collection efficiency of amosite, crocidolite, and chrysotile fibers through the four types of respirator filters

TABLE III. Fiber Size Distribution

	CMD (μm)	σ_{gD}	CML (μm)	σ_{gL}
Amosite	0.18 ± 0.01	1.82 ± 0.11	1.19 ± 0.19	2.32 ± 0.14
Crocidolite	0.083 ± 0.015	1.79 ± 0.07	0.53 ± 0.05	1.68 ± 0.10
Chrysotile	0.030 ± 0.004	1.33 ± 0.13	0.62 ± 0.12	2.15 ± 0.22

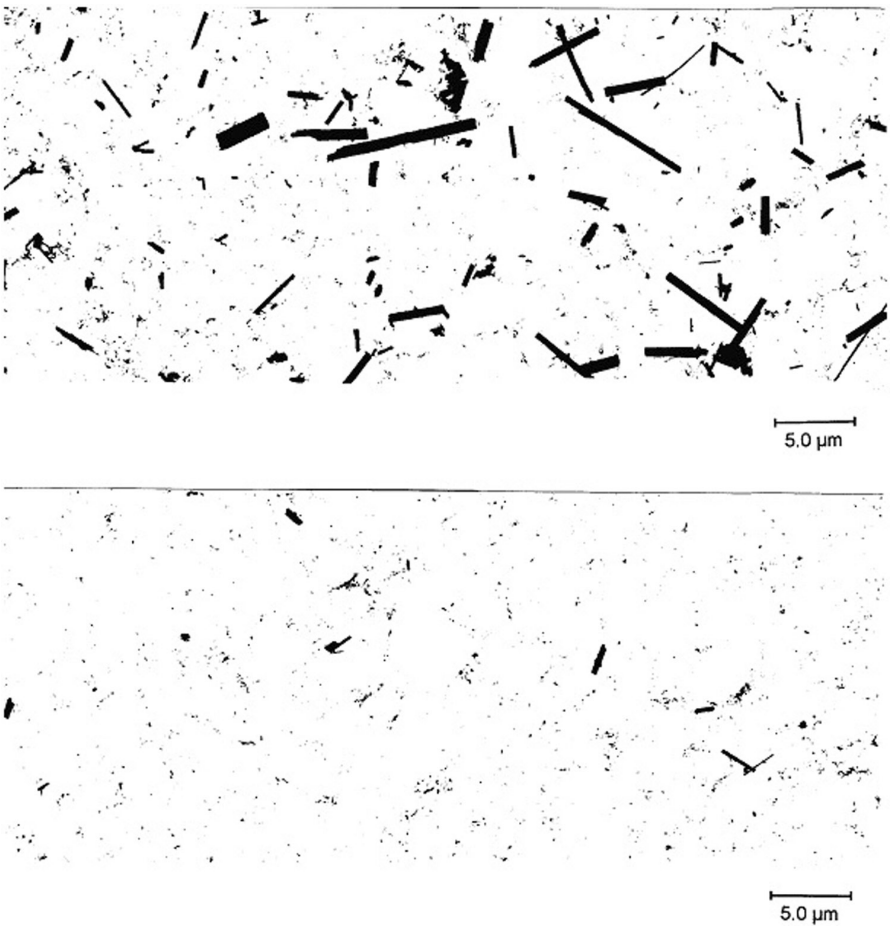

FIGURE 8. Samples of amosite collected upstream (upper panel) and downstream (lower panel) of the test filter cartridge.

are listed in Tables IV–VI, respectively. To estimate the experimental errors, three replicates were performed for the same experimental condition for Filter A using the amosite fiber. The mean collection efficiency and standard deviation are listed in Table IV. The standard deviation was small for data obtained at 32 L min^{-1} but was much higher for data obtained at 85 L min^{-1}. For all other fiber penetration measurements, one test run was performed.

For Filter D no fibers were detected downstream, with the filtration efficiency near 100% (>99.99%) for all three fibers, similar to data obtained for spherical particles. Charge status and flow rate were not a factor in the filtration efficiency. For Filter C, collection efficiency was >98% in all cases. However, there were between 0.02 to 1.1% of fiber penetration in three cases at a flow rate of 32 L min^{-1} (Tables IV and V).

Charge status and flow rates were major factors for filtration efficiency of asbestos fibers for Filters A and B. The most significant effects of the electrostatic charge were observed in the face mask (Filter A), which also had the highest surface potential. Untreated Filter A collected between 94% and 97% of amosite, crocidolite, and chrysotile at a flow rate of 32 L min^{-1}. The efficiency decreased substantially (74% to 80%) when the filter masks were completely neutralized by antistatic spray. The poorest performance was observed at the higher flow rate of 85 L min^{-1} when both the face mask and fibers were discharged. Depositions of 55.0%,

TABLE IV. Amosite Fiber Deposition in the Respirator Filter

Filter Type	Filter Treatment	Flow Rate (L min^{-1})	Fiber Deposition (%)	
			Mean	SD
Filter A	Untreated	32	94.16	0.137
Filter A	Neutralized	32	79.94	0.81
Filter A	Neutralized	85	55.00	12.5
Filter B	Untreated	16	91.37	
Filter B	Neutralized	16	73.16	
Filter B	Neutralized	42.5	97.93	
Filter C	Untreated	32	99.61	
Filter C	Neutralized	32	99.98	
Filter C	Neutralized	85	>99.99	
Filter D	Untreated	16	>99.99	
Filter D	Neutralized	16	>99.99	
Filter D	Neutralized	42.5	>99.99	

TABLE V. Crocidolite Fiber Deposition in the Respirator Filter

Filter Type	Filter Treatment	Flow Rate (L min^{-1})	Fiber Deposition (%)
Filter A	Untreated	32	95.85
Filter A	Neutralized	32	74.08
Filter A	Neutralized	85	29.39
Filter B	Untreated	16	92.57
Filter B	Neutralized	16	88.34
Filter B	Neutralized	42.5	96.92
Filter C	Untreated	32	98.93
Filter C	Neutralized	32	>99.99
Filter C	Neutralized	85	>99.99
Filter D	Untreated	16	>99.99
Filter D	Neutralized	16	>99.99
Filter D	Neutralized	42.5	>99.99

29.4%, and 23.5% were observed using amosite, crocidolite, and chrysotile fibers. This indicates that the electrostatic charges on filter cartridges were major factors in enhancing the collection of asbestos fibers. On the other hand, higher flow rate was associated with further reduction of fiber collection efficiency in the case of neutralized fibers and filter cartridges. A possible explanation was that under these conditions interception and diffusion of the particles were the dominant deposition mechanism for the test filter. Interception and diffusion deposition decreased with increased flow rate.[17]

The performance of Filter B was different from Filter A. The untreated filter collected between 91% and 99% of the amosite, crocidolite, and chrysotile fibers at a flow rate 16 L min^{-1}. The efficiency decreased substantially to between 73% and 95% when the filter was completely neutralized by antistatic spray. However, at 42.5 L min^{-1} for the charged-neutralized filter, the performance returned to higher efficiency (97% to 98%). The results show that the electrostatic charge on filter cartridges was a major factor in enhancing the collection of asbestos fibers. Also, with increased flow rate the collection efficiency also increased slightly, suggesting that the inertial deposition may be a factor.

TABLE VI. Chrysotile Fiber Deposition in the Respirator Filter

Filter Type	Filter Treatment	Flow Rate (L min^{-1})	Fiber Deposition (%)
Filter A	Untreated	32	97.40
Filter A	Neutralized	32	76.81
Filter A	Neutralized	85	23.50
Filter B	Untreated	16	99.50
Filter B	Neutralized	16	95.20
Filter B	Neutralized	42.5	97.99
Filter C	Untreated	32	>99.99
Filter C	Neutralized	32	>99.99
Filter C	Neutralized	85	>99.99
Filter D	Untreated	16	>99.99
Filter D	Neutralized	16	>99.99
Filter D	Neutralized	42.5	>99.99

Comparison of Filter Collection for Spherical and Fiber Aerosol

Our results showed that for HEPA Filter D, the performance of 0.3 μm DEHS particles and three asbestos fibers was essentially the same (>99% collection efficiency). For HEPA Filter C, fiber penetration sometimes exceeded 0.03%, worse than those of the DEHS particles. For Filter A, the collection efficiency of amosite fiber was higher than that for the spherical particles. For crocidolite and chrysotile fibers, the collection efficiencies were higher than for those for the spherical particles at 32 min^{-1}; however, the collection efficiencies were lower than those of the spherical particles at 85 L min^{-1}.

The situation for Filter B was somewhat different. The collection efficiencies were higher in all cases for chrysotile than those of the spherical particles. For both amosite and crocidolite, the fiber collection efficiencies were lower than those of the spherical particles at 16 L min^{-1}, whereas the collection efficiencies were higher at 42.5 L min^{-1}.

CONCLUSIONS

Four different filter types, including a disposable face mask (Filter A) filter, a dust/mist filter (Filter B), a powered respirator HEPA filter (Filter C), and a HEPA filter (Filter D), were tested. Only HEPA filters performed consistently on both spherical test aerosols and three types of asbestos fibers. HEPA Filter D had >99.7% efficiency in all cases. Neither the surface charge potential of the filter cartridges nor the flow rate appeared to affect filter performance. HEPA Filter C showed >99.7% efficiency for DEHS particles but allowed up to 1.1% penetration for asbestos fibers. The performances of the dust/mist filter and disposable face mask deteriorated when the charge potential on the filter was removed or as the flow rate changed.

The surface charge measurements of the respirator filters showed that some filters, including those used in disposable face masks, had high surface charges to enhance the collection efficiency. Our data also showed that the surface charges were decreased in a high-temperature, high-humidity environment and were neutralized within 1 week. Collection of spherical particles and fibers in the charged disposable face mask was enhanced substantially. For Filter B the surface charge was low but measurable. The collection efficiency of spherical particles did show a very small decrease when the filter cartridge of Filter B was neutralized, but it was within the experimental errors. However, the collection efficiency of three asbestos fibers in Filter B decreased substantially when the filter cartridge was neutralized.

A fiber aerosol in charge equilibrium holds more charges than spherical particles,[19–21] and the averaged charge of fiber aerosol is proportional to the fiber length irrespective of fiber diameter.[19–21] In the workplace, higher electrostatic charges were reported for asbestos fiber depending on the sampling location.[21] The electrostatic charge of an aerosol also decreased with time by charge neutralization with free ions in the air.[21] The reported data for asbestos penetration were based on measurements of charge-neutralized fibers. Therefore, the results presented in the study may be considered as the minimum collection efficiency. Higher collection efficiency may be expected for asbestos carrying more electrostatic charges.

In terms of influence of the flow rate on filter cartridge performance, there were no effects for Filters C and D for either spherical or fiber aerosols. For Filter A, the collection efficiency of both spherical particles and fibers decreased as the flow rate was increased from 32 to 85 L min^{-1}.

There was a slight decrease for spherical particle collection on Filter B, but the decrease was within the experimental errors. For asbestos fibers, there was increase in collection for Filter B as the flow rate increased from 16 to 42.5 L min^{-1}. The reason was not clear but may be related to the inertial effects of the collection mechanism.

We conducted the study during the time before the new NIOSH respirator filter regulation was promulgated. The test filters were available at the time but not the new classes of filters. However, we think the results on these test filters are still relevant. Based on our DEHS tests, Filters C and D had performances similar to the N100 filter, and Filter B was similar to the N95 filter.

ACKNOWLEDGMENTS

This research was financially supported by the National Institute for Occupational Safety and Health.

REFERENCES

1. **Stanton, M.F., and C. Wrench:** Mechanisms of mesothelioma induction with asbestos and fibrous glass. *J. Nat. Cancer Inst. 48*:797–821 (1972).
2. **Pott, F., W. Stöber, and K. Spurny:** Properties of asbestos and other fibrous dusts with regard to their carcinogenicity. In *Aerosols in the Mining and Industrial Work Environments*, V.A. Marple and B. Liu (eds.). Ann Arbor, Mich.: Ann Arbor Science, 1983. pp. 585–595.
3. **Cheng, Y.S., Q.H. Powell, S.M. Smith, and N.F. Johnson:** Silicon carbide whiskers: Characterization and aerodynamic behavior. *Am. Ind. Hyg. Assoc. J. 56*:970–978 (1995).
4. **Drew, R., M. Kuschner, and D.M. Bernstein:** The chronic effects of exposure of rats to sized glass fibers. *Ann. Occup. Hyg. 31*:711–729 (1987).
5. **Smith, D.M., L.W. Ortiz, R.F. Archuleta, and N.F. Johnson:** Long-term health effects in hamsters and rats exposed chronically to man-made vitreous fibres. *Ann. Occup. Hyg. 31*:731–754 (1987).
6. **Johnson, N.F., M.D. Hoover, D.G. Thomassen, Y.S. Cheng, A. Dalley, and A.L. Brooks:** In vitro activity of silicon carbide whiskers in comparison to other industrial fibers using four cell culture systems. *Am. J. Ind. Med. 21*:807–823 (1992).
7. **Occupational Exposure to Asbestos:** 29 CFR 1910.1001. 1994. p. 40964.
8. **Cheng, Y.S.:** Bivariate lognormal distribution for characterizing asbestos fiber aerosols. *Aerosol Sci. Technol. 5*:359–368 (1986).
9. **Stöber, W., H. Flachsbart, and D. Hochrainer:** The aerodynamic diameter of latex aggregates and asbestos fibres. *Staub-Reinhalt Luft 30*:1–12 (1970).
10. **Walton, W.H.:** The nature, hazards and assessment of occupational exposure to airborne asbestos dust: A review. *Ann. Occup. Hyg. 25*:148–149 (1982).
11. **Weeks, T.J., and A.F. Burns:** Performance of dust respirators against a fibrous dust. *Am. Ind. Hyg. Assoc. J. 31*:290–293 (1970).
12. **Brosseau, L.M., M.J. Ellenbecker, and J.S. Evans**: Collection of silica and asbestos aerosols by respirators at steady and cyclic flow. *Am. Ind. Hyg. Assoc. J. 51*:420–426 (1990).
13. **Ortiz, L.W., S.C. Soderholm, and S.O. Valdez:** Penetration of respirator filters by an asbestos aerosol. *Am. Ind. Hyg. Assoc. J. 49*:451–460 (1988).
14. *"Respiratory Protective Devices: Test for Permissibility,"* 30 CFR Part 11. 1989. pp. 18–82.
15. **Davis, J.M.G., J. Addison, R.E. Bolton, K. Donaldson, A.D. Jones, and T. Smith:** The pathogenicity of long versus short fiber samples of amosite asbestos administered to rats by inhalation and intraperitoneal injection. *Br. J. Exp. Pathol. 67*:415–430 (1986).
16. **Gentry, J.W., K. Spurny, and J. Schormann:** Collection efficiencies of ultrafine asbestos fibers: Experimental and theory. *Aerosol Sci. Technol. 11*:184–195 (1989).
17. **Lee, K.W., and B.Y.H. Liu**: On the minimum efficiency and the most penetrating particle size for fibrous filters. *J. Air Pollut. Contr. Assoc. 30*:377–381 (1980).
18. **Chen, B.T., H.C. Yeh, and B.J. Fan:** Evaluation of the TSI small-scale powder disperser. *J. Aerosol Sci. 26*:1303–1313 (1995).
19. **Cheng, Y.S., and H.C. Yeh:** Theoretical equilibrium charge distributions of chain aggregates with uniform spheres. *J. Aerosol Sci. 14*:489–494 (1983).
20. **Vincent, J.H., W.B. Johnston, A.D. Jones, and A. M. Johnston:** Static electrification of airborne asbestos: A study of its causes, assessment and effects on deposition in the lungs of rats. *Am. Ind. Hyg. Assoc. J. 42*:711–721 (1981).
21. **Johnston, A.M., J.H. Vincent, and A.D. Jones:** Measurements of electric charge for workplace aerosols. *Ann. Occup. Hyg. 29*:271–284 (1985).